FeC_n^- and FeC_nH^- (n=3,4): A photoelectron spectroscopic and density functional study

Jiawen Fan
Environmental Molecular Sciences Laboratory, Pacific Northwest Laboratory, MS K2-14, Richland, Washington 99352

Liang Lou
Rice Quantum Institute and Departments of Chemistry and Physics, Rice University, Houston, Texas 77251

Lai-Sheng Wang[a)]
Environmental Molecular Sciences Laboratory, Pacific Northwest Laboratory, MS K2-14, Richland, Washington 99352, and Department of Physics, Washington State University, Richland, Washington 99352

(Received 17 August 1994; accepted 8 November 1994)

Photoelectron spectra of the title molecules are reported at 3.49 eV photon energy. Vibrational structures are resolved in the spectra of FeC_3^- and FeC_3H^-. The FeC_4^- spectrum is unusually broad, indicating a large equilibrium geometry change from the anion to the neutral states. The FeC_4H^- spectrum exhibits a single strong feature. Theoretical studies using the density functional theory are carried out to determine the structures and bonding of these clusters. All the molecules in the anion ground states are found to be linear with the Fe atom bonded at one end. The Fe and C bonding involves strong Fe 4*s* and C *sp* interactions as well as considerable Fe 3*d* and C π interactions. The $n=3$ species can be best characterized by cumulenic types of bonding with FeC_3H also having an acetylenic isomer. The $n=4$ species in the linear structures can be approximately described by diacetylenic types of bonding. Mulliken charge analyses indicate that the extra charge in all the anions enters mainly into the Fe 4*s* antibonding orbital, in agreement with the assignment that the threshold detachment takes place from the σ^* orbital mainly between the Fe and C atoms. The vibrational structure resolved in the FeC_3^- spectrum yields a Fe–C stretching frequency of 700 (150) cm^{-1} for the first excited state of FeC_3, in agreement with the Fe–C multiple bonding character. © *1995 American Institute of Physics.*

I. INTRODUCTION

The first row transition metals exhibit a wide range of interactions with carbon. This is not only reflected in their bulk carbide properties, but also in smaller systems. For example, early transition metals are found to easily form met–cars,[1] a series of apparently stable and pure metal–carbon molecules with a definitive stoichiometry ($Ti_8C_{12}^+$ is a typical example), while late transition metals have less tendency to do so.[2] Furthermore, very recently several late transition metals have been found to be catalysts for single carbon nanotube formation.[3,4] Although the chemistry of the transition metals can be qualitatively explained by the difference of the *d* orbitals across the periodic table, these novel findings of the carbon chemistry with transition metals are not well understood. To elucidate the detailed interactions between the transition metals and carbon, we have initiated a study of the electronic structures of small transitions metal/carbon clusters by anion photoelectron spectroscopy (PES), which can provide unique information about the chemical bonding of these clusters.

Furthermore, small carbon and hydrocarbon fragments are important intermediates for hydrocarbon dehydrogenation on transition metal catalysts.[5] Small clusters of these fragments with transition metals may provide good model compounds to understand the complex catalytic reactions taking place on the catalyst surfaces. We have briefly reported our results on FeC_2^- and FeC_2H^-, which are interpreted based on an acetylenic-type bonding with a CC triple bond.[6] In a very interesting recent work,[7] Bowers *et al.* have measured the ion mobility of a series of $Fe_xC_y^-$ clusters and have discussed the possible structural and bonding configurations of this class of clusters. They have also performed *ab initio* calculations on these clusters.[8] For the $x=1$ series, they find that FeC_4^- has a single isomer, consistent with a linear structure. For $x=1$ and $y>4$, they observe that more than one isomer can be populated in the anion, consistent with a linear and a ring type of structure. In this article, we present the first photoelectron spectroscopic study on FeC_n^- and FeC_nH^- ($n=3,4$) from our recently built high resolution magnetic-bottle time-of-flight photoelectron apparatus.[9]

Density functional theory (DFT) calculations are performed for all the clusters. These calculations not only help the interpretation of the experimental PES spectra, but also provide key insights into the cluster structures and bonding. All the negative ions are found to be linear in the nonlocal corrected level in the DFT calculations. Three isomers with close energies are found for FeC_3H^-. Significant structural change is indicated from the anion to the neutral from the diffusiveness of the FeC_4^- spectrum. Vibrational structures are observed for FeC_3^- and FeC_3H^-. The large Fe–C vibrational frequencies are in agreement with the formation of multiple Fe–C bonds.

a)To whom correspondences should be addressed.

II. EXPERIMENT

The $Fe_xC_yH_z^-$ anions are generated by laser vaporization of an iron target with a He carrier gas containing 5% CH_4. The $Fe_xC_y^-$ clusters can also be produced by vaporizing a Fe/C target pressed from Fe/C powders. The photoelectron spectrometer used in this study[9] is a newly modified version of a magnetic-bottle time-of-flight (TOF) photoelectron analyzer.[10] Details of the apparatus will be published elsewhere;[9] only a brief description of the experimental procedure is presented here. The second harmonic output from a Q-switched Nd:YAG laser operated at 10 Hz is used for the laser vaporization. The laser beam (10 mJ/pulse) is focused to a 1 mm diameter spot onto an iron target that is driven by two computer-controlled stepping motors. The carrier gas, containing 5% methane in He at 6.5 atm total pressure, is delivered by two pulsed molecular beam valves (R. M. Jordan, Co.) and is synchronized with the vaporization laser pulse. The plasma reactions of CH_4 and Fe produce a variety of cluster species which, together with the He carrier gas, undergo a supersonic expansion and are skimmed twice to form a collimated beam. About 70 cm down stream from the cluster nozzle, the negative cluster ions are extracted by a 1 kV high voltage pulse into a 130 cm long flight tube for mass analyses. The TOF mass spectrometer has a large extraction volume and a modified Wiley–McLaren extraction stack with an added free-flight region between the two acceleration stages.[11] It has a mass resolution ($M/\Delta M$) of more than 300, sufficient to resolve all the isotopic species in the mass range pertinent to the current study.[9]

A three-grid mass gate is used to select only the desired clusters to enter the PES interaction zone. The mass-selected cluster anion packet is decelerated by a new momentum deceleration procedure[9] down to a very low velocity before photodetachment in order to minimize the Doppler broadening on the photoelectron kinetic energy distribution. This is crucial to achieve high energy resolution with the magnetic bottle-type photoelectron analyzer. The third harmonic of a second Q-switched Nd:YAG laser is used for the photodetachment. The spectrometer is calibrated with the known spectrum of Cu^-. The energy resolution (ΔE) in a TOF spectrometer is not constant with respect to the electron kinetic energy (Ek); ΔE is proportional to $Ek^{3/2}$. An energy resolution of 30 meV at 1 eV electron kinetic energy is achieved in the current spectrometer with the new deceleration procedure, as measured from the photoelectron spectrum of Cu^- at 3.49 eV photon energy.

III. DENSITY FUNCTIONAL CALCULATIONS

Density-functional calculations are performed to determine the equilibrium structure of these iron–carbon clusters. The cluster geometries are optimized within the local density approximation (LDA) framework[12] using the von Barth–Hedin spin-polarized exchange-correlation potential.[13] Nonlocal corrections are included in the final evaluation of total energy. Becke's formulation of nonlocal exchange potential is used.[14]

The Kohn–Sham equations for the electronic system are expanded in linear combination of atomic orbitals and solved variationally using three-dimensional integration methods.[14,15] The orbital functions used in the calculations are numerical solutions of spherical atoms and ions. For iron, the basis set includes all the occupied atomic orbitals of the Fe atom and the valence orbitals of an Fe^{2+} ion, plus the ionic $4p$ orbital as a polarization function. The basis sets for carbon and hydrogen are similarly constructed, except that a d-type polarization function is used for carbon and the ion used for hydrogen is $He^{1.3+}$. This type of double numerical basis[15] has been used previously for clusters involving $3d$ transition metals and carbon and has shown to yield very satisfactory results for these kinds of systems.[16]

The calculated total energy (presented as the relative energy between different structures for each cluster), the population on the Fe $3d/4s$ orbitals based on a Mulliken analysis, and the bond lengths in each structure are listed in Table I. Both the linear and two-dimensional structures are obtained by minimizing the total energy using analytical gradient methods, with no symmetry constraints on the displacements of the nuclei. The final structures show obvious symmetrical atomic arrangements. The point group symmetry associated with each structure is indicated in the table.

Due to the existence of low-lying excited states, small amounts of different states have to be mixed in to help facilitate the convergence of the self-consistent procedure for solving the Kohn–Sham equations.[17] The total energy thus obtained might be slightly higher than that of the true ground state. The uncertainty introduced this way is estimated to be in the order of 0.01 eV. In most cases, this is about one to two orders of magnitude smaller than the energy difference between different structures, as shown in Table I.

Small carbon clusters prefer linear atomic arrangements, which are expected to be a good starting point for the FeC_n and FeC_nH clusters considered presently. Additionally, bent and ring-like structures are also possible candidates and have been carefully considered and examined. For the FeC_n clusters, the ring structure is formed by closing a linear chain of iron and carbon atoms. For the FeC_nH clusters, the ring structure is obtained by attaching the H atom to one of the carbon atoms on the FeC_n ring. Different C sites for the H attachment have been compared before the lowest energy ring structure of an FeC_nH cluster is determined.

In all the cases, the linear chain structure is found to be the most stable at the nonlocal exchange corrected level of our calculations. At the LDA level, the two-dimensional structures tend to be in lower energy. The reversal of relative energy by including the nonlocal corrections indicates the significance of more accurate evaluation of exchange (and correlation) potential energy in this type of calculation. The difference made by inclusion of the gradient corrections is possibly due to two factors: (1) the relatively large spatial variations of electron density in the multiple bonding regions, the existence of which are typical to the iron–carbon clusters considered here; and (2) the alignment of d electrons, which can lead to a local magnetic moment of nearly 3 μ_B at the Fe site when a linear chain structure is formed with the iron at one end, and in this case, a large local spatial change in spin density is expected. However, in the ring structure, the Fe atom is bonded to more than one carbon

TABLE I. Density-functional calculations of FeC_n, FeC_n^-, FeC_nH, and FeC_nH^- (n=3,4).

		ΔE^{LDA}[a]	ΔE^{NL}[a]	$Q(3d/4s)$[b]	R (Fe–C)[c]	R (C–C)[d]
FeC_3	linear ($C_{\infty v}$)	0.77	0.00	6.76/0.85	1.665	1.304, 1.293
	ring (C_{2v})	0.00	0.21		1.753	1.359
					1.752	1.359
FeC_3^-	linear ($C_{\infty v}$)	0.42	0.00	6.91/1.43	1.622	1.336, 1.281
	ring (C_1)	0.00	0.45		1.768	1.394
					1.771	1.392
FeC_3H	linear ($C_{\infty v}$)	−0.35	0.00	6.82/1.08	1.623	1.343, 1.234
	ring (C_1)	0.00	0.97		1.722	1.441
					1.718	1.441
FeC_3H^-	linear ($C_{\infty v}$)	0.74	0.00	6.92/1.60	1.633	1.338, 1.254
	ring (C_{2v})	0.00	−0.04		1.726	1.445
					1.726	1.445
FeC_4	linear ($C_{\infty v}$)	0.28	0.00	6.69/0.79	1.722	1.274, 1.309, 1.291
	ring (C_{2v})	0.00	1.11		1.829	1.350, 1.333
					1.829	1.333
FeC_4^-	linear ($C_{\infty v}$)	0.20	0.00	6.70/1.40	1.741	1.267, 1.336, 1.275
	ring (C_{2v})	0.00	0.80		1.911	1.394, 1.300
					1.910	1.300
FeC_4H	linear ($C_{\infty v}$)	−0.06	0.00	6.71/0.94	1.755	1.250, 1.339, 1.226
	ring (C_1)	0.00	1.07		1.772	1.412, 1.298
					1.841	1.361
FeC_4H^-	linear ($C_{\infty v}$)	−0.32	0.00	6.73/1.63	1.714	1.267, 1.336, 1.242
	ring (C_1)	0.00	1.30		1.724	1.422, 1.293
					1.874	1.386
$FeCH_3$					1.891	
$FeCH_2$					1.722	
FeCH					1.579	

[a]Total energy difference between the two cluster structures in eV; LDA: local density approximation; NL: nonlocal gradient corrected.
[b]Mulliken charges on the Fe 3d and 4s orbitals for the linear structures.
[c]Fe–C bond length in Å. There are two Fe–C bonds for the ring structures.
[d]C–C bond length in Å. For the linear structure, the first number is the C–C bond closest to the Fe atom and in that order. For the n=4 ring structures, the number in the second row is the C–C bond further away from the Fe atoms.

atom and, therefore, the spin alignment at the iron site will be reduced.[18]

The linear chain structures obtained here are consistent with the ion mobility experiments of Bowers *et al.*[7] on FeC_4^-, for which only one isomer is found. They conclude that it has a linear chain structure, which is also supported by their *ab initio* calculations.[8]

As a comparison, we also perform calculations on $FeCH_3$, $FeCH_2$, and FeCH, which have been studied previously by various theoretical methods[19–21] and are known to form single, double, and triple Fe–C bonds, respectively. The Fe–C bond lengths from the LDA calculations, shown in Table I, are slightly shorter than those given in previous calculations. Nevertheless, the Fe–C bond lengths in $FeCH_3$, $FeCH_2$, and FeCH can serve as references for the Fe–C bond lengths in the FeC_n and FeC_nH species. By comparison, the Fe–C bonds in all the FeC_n and FeC_nH clusters have some multiple bonding character, including the strong Fe 3d interactions with the π orbitals on the C_n and C_nH fragments. Additionally, it can be seen that the Fe–C bonds are shorter in those with n=3 than those with n=4, indicating a stronger Fe–C bond for n=3. This is because for n=4, the four C atoms can form a diacetylenic type of bonding, reducing the tendency for Fe–C multiple bonding. There is a certain degree of electron delocalization, smearing out the formal bond orders. The bonds between Fe–C and C–C at the two ends of the chain have some ionic character. For example, in the neutral chain of FeC_4, the Mulliken charge at the Fe site is $+0.3e$ and that at the C site in the opposite end is $-0.2e$. The same is true for the FeC_3. For the neutral species, it can be seen from the Mulliken charges (Table I) that the Fe atom is mainly in a $3d^74s^1$ configuration in the cluster bonding. For the anion, the extra charges are mostly deposited on the Fe site ($0.6e$) entering mainly into the 4s orbitals. This will be important for the interpretation of the PES spectra.

The FeC_3H^- has two other isomers that are very close in energy besides the linear one depicted in Fig. 1: a ring structure and a linear structure where the H atom is 20° off linear.

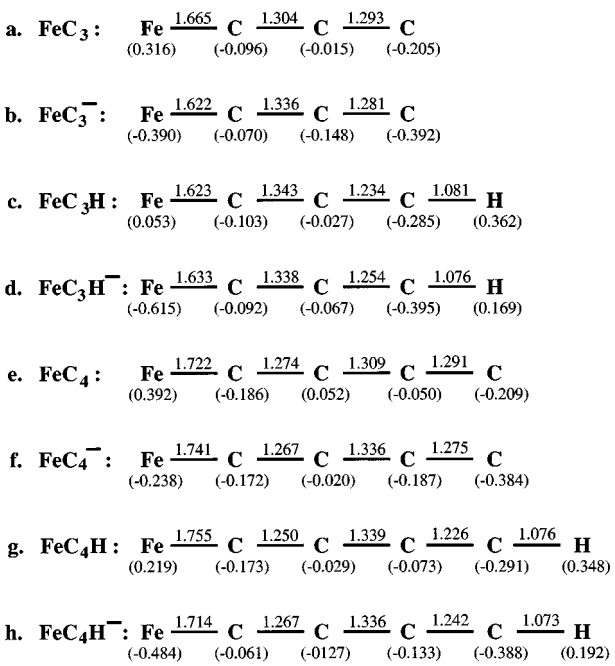

FIG. 1. Structures and Mulliken charges of the FeC_n, FeC_nH, FeC_n^-, and FeC_nH^- (n=3,4) from the LDA calculations. The numbers is parentheses are the Mulliken charges, the numbers between the atoms are the bond lengths in Å.

The latter isomer is much like a cumulenic FeC_3H^- in which the terminal C atom is sp^2 hybridized.

IV. RESULTS AND DISCUSSION

The PES spectra of FeC_3^- and FeC_4^- are shown in Fig. 2; their singly hydrogenated species are shown in Fig. 3. Two prominent bands, labeled X and A, are observed for the spectra of FeC_3^- and FeC_3H^-. Vibrational structures are resolved for the A band in both spectra, as indicated in the figures. They both consist of one major vibrational progression. The X band contains unresolved vibrational features. The very fine features in the spectra are due to the statistical noise. In the spectrum of FeC_3H^-, less prominent features (a and b) are also observed. As will be discussed later, these suggest the presence of more than one isomer in the FeC_3H^- beam. A single strong feature (X) is observed for the spectrum of FeC_4H^- with a weak feature at about 2.8 eV binding energy. The spectrum of FeC_4^- is surprisingly diffuse with less well-defined features. This is dramatically different from the spectra of the other species. The electron affinities (EAs) are determined from the first feature in the photoelectron spectra. Due to the broadness of its spectrum, only an estimate of the photodetachment threshold is possible for FeC_4 as indicated by the arrow in Fig. 2. This threshold value can be consid-

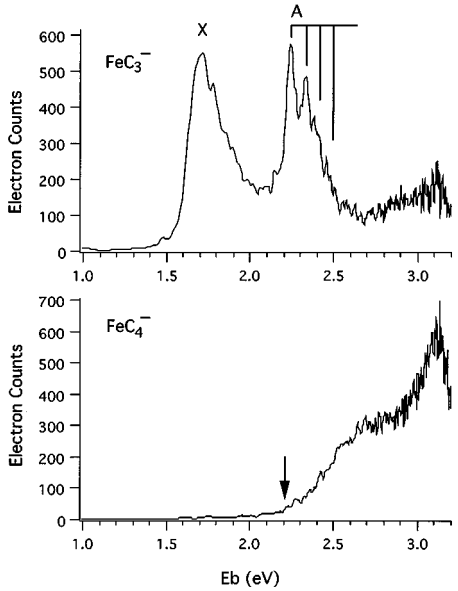

FIG. 2. Photoelectron spectra of FeC_3^- and FeC_4^- at 3.49 eV photon energy. The arrow in the FeC_4^- spectrum indicates the detachment threshold.

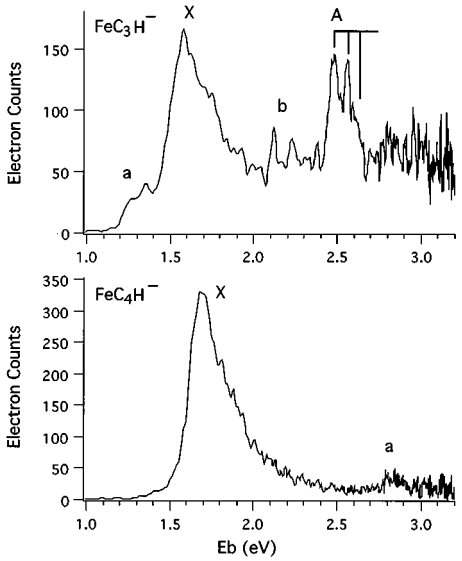

FIG. 3. Photoelectron spectra of FeC_3H^- and FeC_4H^- at 3.49 eV photo energy.

TABLE II. Spectroscopic constants and energies of FeC_n and FeC_nH (n =3,4), obtained from their anion photoelectron spectra.

	FeC_3	FeC_3H		FeC_4H	FeC_4
		I[a]	II[b]		
EA (eV)[c]	1.69(8) (X)	1.58(6) (X)	1.27(8) (a)	1.67(6) (X)	2.2(2)
Excited state[d] (eV)	2.25(4) (A)	2.48(5) (A)	2.12(5) (b)	2.82(7) (a)	
ν_{Fe-C} (cm^{-1})	700(150)	670(150)	880(150)		

[a]The cumulenic isomer.
[b]The acetylenic isomer.
[c]The electron affinity as determined from the threshold band maxima. The value for FeC_4 as indicated by the arrow in Fig. 1 is the photodetachment threshold, which can be taken as the upper bound of the adiabatic EA.
[d]In term of the electron binding energy. The term value is obtained by subtracting the EA from this number.

ered as the upper bound of the adiabatic EA. The other features at higher binding energies represent the excited states of the neutral species. The energies and spectroscopic constants obtained for the four clusters are listed in Table II.

Photodetachment takes place from the ground state of an anion to the ground state and the various excited states of the neutral at the same nuclear configuration as the anion. When the neutral has similar equilibrium geometry as the anion, a rather sharp PES spectrum is expected as a result of the vertical transition. However, if the neutral has a different equilibrium geometry than the anion, broad spectrum with extensive vibrational excitations is expected due to the Frank–Condon envelope. The excited states of the clusters are more difficult to obtain. Thus, the PES spectrum is usually interpreted based on the single-electron approximation by using the molecular orbital argument. This is quite effective and can account for the main PES features. We will interpret the PES spectra of the FeC_n^- and FeC_nH^- species based on bonding properties of these species obtained from the LDA calculations and simple molecular orbital considerations.

The structure and bonding of the FeC_n and FeC_nH clusters as described by the above LDA calculations are quite reasonable. In the case of FeC_4^-, the predicted structure is in agreement with the ion mobility experiment.[7] The linear structures obtained for these small clusters all have a terminal Fe–C bond. Such an atomic arrangement is also in accordance with our chemical intuitions. The C–C bond is known to be much stronger than the Fe–C bond.[19,20] Thus, it is not energetically favorable for Fe to insert into the C chain since that will break the stronger C–C bonds and form the weaker Fe–C bonds. The Fe atom has a $3d^6 4s^2$ (^5D) ground state configuration with an excited state (^5F, $3d^7 4s^1$) 0.9 eV higher in energy.[22] The LDA calculations indicate that in all the FeC_n and FeC_nH clusters the excited Fe atom is involved in the chemical bonding. In a linear geometry, simple molecular orbital considerations suggest that the C atom directly bonded to the Fe atom must be in an sp hybridized state in order to more effectively interact with the Fe $4s$ orbital. And the Fe $3d$ orbitals can interact with the other p orbitals on the C atoms to form additional bonds. This bonding character is well depicted by the LDA calculations. In the following, we will discuss each species separately.

A. FeC_3^-

The C_3 molecule has been well studied and is known to be linear with the singlet ground state.[23,24] It can be viewed to have a cumulenic type of bonding with two lone pairs on the terminal carbon atoms (:C═C═C:). The excited Fe atom will form a $(3d^7\text{-}p^1)\sigma^2\sigma^{*0}$ FeC_3 with an excited C_3, where $(3d^7\text{-}p^1)$ depicts a strong π interaction between the C p orbitals and the Fe $3d$ orbitals, σ and σ^* are the $4s\text{-}sp$ bonding and antibonding orbital, respectively. Hence, the anion FeC_3^- will have a $(3d^7\text{-}p_x^1)\sigma_{sp}^2\sigma^2\sigma^{*1}$ configuration with the extra electron entering the σ^* antibonding orbital. This is in agreement with the Mulliken population analysis of the LDA molecular orbitals for this cluster, showing that, like in the other anionic clusters being considered, the extra electron enters mainly into the Fe $4s$ orbital (see Table I).

The two main features of the FeC_3^- spectrum exhibit vibrational structures that are well resolved in the A band. This suggests that the electrons removed in both states are either bonding or antibonding. We assign the X band to be from the removal of the least-bound σ^* antibonding electron and the A band to the removal of a σ bonding electron. The vibrational frequency of 700(150) cm^{-1} in the A band is in fair agreement with the Fe═C stretching in Fe═CH_2 observed in a previous matrix study[25] and is much higher than that for a Fe–C single bond.[6] This is also in agreement with the LDA calculations that yield a Fe–C bond length indicative of a multiple Fe–C bond.

B. FeC_3H^-

The complex appearance of the FeC_3H^- spectrum suggests that there may be more than one isomer present in the anion beam. Indeed, the LDA calculations predict that FeC_3H^- has at least three isomers that are close in energy: the linear one as shown in Fig. 1, a cumulenic isomer in which the H atom is off linear by 20° (Fe═C═C═C–H), and a ringlike isomer. The two linear forms of FeC_3H^-, with different H off-line angles, are almost degenerate in energy. The two-dimensional ring structure is sightly lower in energy by only 0.04 eV with nonlocal exchange corrections included. The FeC_3H^- PES spectrum suggests that at least there can be two isomers; one associated with the two major bands X and A; one associated with the two smaller features a and b, as shown in Fig. 3. The ring isomer is quite unusual and has a very different electronic structure from the linear isomers. We assign the spectrum to be due to the first two isomers. The difference between the two is subtle. The linear one is more like an acetylenic type where the H atom is bonded to an sp hybridized C atom and the Fe–C bond length is close to a triple bond. In the cumulenic isomer, the H atom is bonded to a sp^2 hybridized C atom and the Fe–C bond is close to a double bond. The bond length and the Mulliken charges are really quite similar in both isomers. They are only different by the positions of the H atom.

The X and A bands are rather similar to that in the FeC_3^- spectrum. The vibrational frequency of 670(150) cm^{-1}, observed in the A band, is also very close to that as observed in the A band of the FeC_3^- spectrum. We assign these to the cumulenic isomer whose bonding should be quite similar to that in FeC_3. And the two bands are due to the removal of a $4s\text{-}sp$ antibonding and bonding electron, respectively. The assignment of the X band to the removal of the σ^* electron is supported by the LDA calculations that indicate the extra electron enters this antibonding orbital in the anion. The observed vibrational structure in the A band is consistent with removal of a bonding electron; the large vibrational frequency is in accordance to a multiple Fe–C bond.

The b band exhibits a vibrational structure with a frequency of 880(150) cm^{-1}. We assign the a and b bands to the linear acetylenic isomer of FeC_3H^-. The two features result from the removal of the $4s\text{-}sp$ σ^* and σ electrons, respectively. The vibrational structure is due to the Fe–C stretching. The rather high frequency displayed in the b band

suggests that the Fe–C bond is stronger in this isomer, in excellent agreement with the fact that the Fe–C bond should have a triple bond character.

C. FeC_4^-

The spectrum of FeC_4^- is very diffuse and is dramatically different from the other spectra. This indicates that there is a large difference in equilibrium geometry between the neutral states and the ground state of the anion. The FeC_4^- anion has a linear structure, which is concluded from both the current LDA calculations and the ion mobility experiments and *ab initio* calculations of Bowers *et al.*[7,8] Therefore, the FeC_4 neutral either has quite different bond lengths in a linear structure or has a different structure. The current LDA calculations indicate that FeC_4 neutral is linear and that the bond lengths do not change dramatically from that of the anion. Thus, if FeC_4 were to have a linear structure, then its corresponding PES spectrum should not be so diffuse. Nevertheless, the LDA calculations do not predict a bent or ring structure for this cluster.

The ion mobility experiments indicate the FeC_n^- for $n>4$ can have both linear and ring types of isomers. The anion FeC_4^- does not have a ring isomer presumably due to the strain energy of its relatively small size. However, preliminary *ab initio* calculations by Bowers *et al.*[8] suggest that for the FeC_4 neutral the ring structure is more stable than the linear one by 9 kcal/mol and in FeC_6 the ring structure is more stable than the linear one by 25 kcal/mol. Since both experiment and theories have predicted that the FeC_4^- anion is linear, we tentatively assign the spectrum to be due to a structural change in the neutral.

D. FeC_4H^-

The FeC_4H^- spectrum shows only one strong band, nearly identical to that of FeC_2H^-, which has been shown to have an acetylenic structure (Fe–C≡C–H) with a $3d^7\sigma^2\sigma^{*1}$ configuration.[6] The σ and σ^* are the bonding and antibonding orbitals between the Fe $4s$ and C sp. The single strong band is from the removal of the σ^* electron from the anion. The LDA calculations indicate that FeC_4H^- is linear with a similar diacetylenic structure. The electronic structure of a diacetylenic FeC_4H is expected to be quite similar to that of an acetylenic FeC_2H; and the major bonding interaction is between the Fe $4s$ and the C sp. A Mulliken analysis for the LDA calculations of FeC_4H^- suggests that the extra charge in the anion mainly enters the σ^* orbital. Therefore, we assign the single strong band to be from the removal of the $4s$-sp antibonding σ^* electron from the FeC_4H^- anion. The width of this band indicates some vibrational excitation of the Fe–C stretching, which is partially resolved in the FeC_2H^- case at a 532 nm detachment wavelength.[6]

The weak feature, labeled *a* in Fig. 3, is also very similar to that as in the FeC_2H^- spectrum. There may also be a weak feature unresolved in the high energy tail on the *X* band, as is the case in FeC_2H^-.[6] These features are likely to be due to the Fe $3d$ electrons, which are known to have low detachment cross sections.[26] However, from the weakness of these features, they can also be due to multielectron processes as a result of strong electron correlation effects.[27] These processes are not commonly observed, but they may take place in systems involving transition metals due to the strong electron correlation effect of the *d* electrons.

We also obtained the spectrum of FeC_4D^-, which is identical to the spectrum of FeC_4H^-. The small zero point energy shift in the electron affinity cannot be distinguished in our spectra.

V. SUMMARY

In summary, we have obtained the photoelectron spectra of FeC_n^- and FeC_nH^- for $n=3$ and 4 for the first time. Vibrational structures are resolved for the $n=3$ species and are very useful in elucidating the bonding of the molecules. Density functional theory calculations are performed on all the clusters. The anions are all found to be linear with the Fe atom bonded to a C atom at one end. In the hydrogenated species, the H atom prefers to be on the other end of the chain. Several isomers are found for FeC_3H^-, in agreement with the PES spectrum that suggests the existence of isomers. The spectrum is assigned to be due to a cumulenic and an acetylenic isomer. FeC_4H is found to have a diacetylene type of structure. FeC_3 can be best characterized to have a cumulenic type of bonding. The FeC_4^- spectrum shows very broad features, suggesting a large geometry change from the anion to the neutral.

The bonding between the Fe atom and the carbon and hydrocarbon fragments are highly interesting. Further studies will be focused on larger Fe/C clusters to elucidate their electronic and geometric structures. Met–car forms of Fe/C clusters have been observed,[2] but they are much less prevalent than those for the early transition metals. Transition metal endohedral fullerenes are also known to be quite difficult to synthesize. This is likely to be due to the nature of the interaction between the transition metals and the small carbon fragments. It would also be interesting to study the small transition metal/carbon clusters across the periodic table to elucidate the structural and bonding changes for the different M/C clusters. The properties of these small clusters should provide insight as to what forms of the larger clusters can be expected, as well as the catalytic roles of the transition metals in the carbon nanotube formation.

ACKNOWLEDGMENTS

L.S.W. would like to thank Dr. S. D. Colson and Dr. John Lineham, for valuable discussions. He is particularly grateful to Professor M. T. Bowers and Dr. P. Matire for valuable discussions and for communicating their experimental and theoretical results prior to publication. This work was performed at Pacific Northwest Laboratory, a multiprogram national laboratory operated for the U. S. Department of Energy by Battelle Memorial Institute under Contract No. DE-AC06-76RLO 1830.

[1] B. C. Guo, K. P. Kerns, and A. W. Castleman, Science **255**, 1411 (1992).
[2] J. S. Pilgrim and M. A. Duncan, J. Am. Chem. Soc. **115**, 6958 (1993).
[3] S. Iijima and T. Ichihashi, Nature **363**, 603 (1993).
[4] D. S. Bethune, C. H. Kiang, M. S. de Vries, G. Gorman, R. Savoy, J. Vaquez, and R. Beyers, Nature **363**, 605 (1993).

[5] See, for example, G. A. Somorjai, *Introduction to Surface Chemistry and Catalysis* (Wiley, New York, 1994), p. 406.
[6] J. Fan and L. S. Wang, J. Phys. Chem. **98**, 11814 (1994).
[7] G. von Helden, N. G. Gotts, P. Maitre, and M. T. Bowers, Chem. Phys. Lett. (submitted, 1994).
[8] P. Maitre, G. von Helden, and M. T. Bowers (to be submitted).
[9] L. S. Wang, H. S. Cheng, and J. Fan, J. Chem. Phys. (submitted, 1994).
[10] (a) P. Kruit and F. H. Read, J. Phys. E **16**, 313 (1983); (b) O. Cheshnovsky, S. H. Yang, C. L. Pettiette, M. J. Craycraft, and R. E. Smalley, Rev. Sci. Instrum. **58**, 2131 (1987).
[11] W. A. de Heer and P. Milani, Rev. Sci. Instrum. **62**, 670 (1991).
[12] (a) W. Kohn and L. J. Sham, Phys. Rev. A **140**, 1133 (1965); (b) R. O. Jones and O. Gunnarsson, Rev. Mod. Phys. **61**, 689 (1989).
[13] U. von Barth and L. Hedin, J. Phys. C **5**, 1629 (1972).
[14] A. D. Becke, Phys. Rev. A **38**, 3098 (1988).
[15] (a) A. D. Becke, J. Chem. Phys. **88**, 2547 (1988); (b) B. Delley, J. Chem. Phys. **92**, 508 (1990).
[16] L. Lou and P. Nordlander, Chem. Phys. Lett. **224**, 439 (1994).
[17] This is done by allowing fractional occupations for the molecular states near the highest occupied levels. The fractional occupation numbers are determined using a Fermi-distribution function with the temperature set for less than 50 K.
[18] J. L. Chen, C. S. Wang, K. A. Jackson, and M. R. Pederson, Phys. Rev. B **44**, 6558 (1991).
[19] M. L. McKee, J. Am. Chem. Soc. **112**, 2601 (1990).
[20] C. W. Bauschlicher, S. R. Langhoff, H. Partridge, and L. A. Barnes, J. Chem. Phys. **91**, 2399 (1989).
[21] E. A. Carter and W. A. Goddard, III, J. Am. Chem. Soc. **108**, 2180 (1986).
[22] C. E. Moore, *Atomic Energy Levels*, National Bureau of Standard Circular, Vol. II (U.S. GPO, Washington, D.C., 1971).
[23] K. Raghavachari, Chem. Phys. Lett. **171**, 249 (1990), and references therein.
[24] W. Weltner and R. J. Van Zee, Chem. Rev. **89**, 1713 (1989).
[25] S. C. Chang, Z. H. Kafafi, R. H. Hauge, W. E. Billups, and J. L. Margrave, J. Am. Chem. Soc. **107**, 1447 (1985).
[26] P. C. Engelking and W. C. Lineberger, Phys. Rev. A **19**, 149 (1979).
[27] S. T. Lee, S. Suzer, E. Mathias, R. A. Rosenberg, and D. A. Shirley, J. Chem. Phys. **66**, 2496 (1977).